DESIGN AND ANALYSIS APPROACH FOR LINEAR AEROSPIKE NOZZLE

Safwan Ullah Khan,*
*Abid Ali Khan**† &*
*Adnan Munir**

ABSTRACT

The paper presents an aerodynamic design of a simplified linear aerospike nozzle and its detailed exhaust flow analysis with no spike truncation. Analytical method with isentropic planar flow was used to generate the nozzle contour through MATLAB®. The developed code produces a number of outputs comprising nozzle wall profile, flow properties along the nozzle wall, thrust coefficient, thrust, as well as amount of nozzle truncation. Results acquired from design code and numerical analyses are compared for observing differences. The numerical analysis adopted an inviscid model carried out through commercially available and reliable computational fluid dynamics (CFD) software. Use of the developed code would assist the readers to perform quick analysis of different aerodynamic design parameters for the aerospike nozzle that has tremendous scope of application in future launch vehicles.

Keywords: *Rocket Propulsion, Aerospike Nozzle, Contour Design, Computational Fluid Dynamics*

1. INTRODUCTION

In order to develop an optimum propulsion system and realize the human dream of space exploration, different aspects of aerospike engine are under active research since 1950's. Scientists involved with rocket propulsion have known the fact that an aerospike engine has the highest potential for significantly improving the overall performance of satellite launch vehicles through all phases of flight (Tirpak and John, 1998; Dorsey, et al., 1999; Bradford, et al., 2000; Garvey and Besnard, 2004; Bui, et al., 2005). An extraordinary performance, integrated over the flight time, is especially important for high velocity missions, such as the single stage to orbit (SSTO) application (Sutton and Biblarz, 2011). One such proposed SSTO vehicle is X-33 with a linear Aerospike nozzle (Jackson, et al., 1998; Wang, 1999; Shtessel and Hall, 2000). A simplified aerospike nozzle geometry is shown in Figure-1. Unlike conventional nozzles, in which performance losses occur especially at lower altitudes as the engine is designed to have an optimum thrust at only one design altitude, aerospike is believed to recover up to 50 percent of those losses (Huebner, et al., 1995). The recovery is possible due to its unique ability of compensating for the varying altitudes (and thus varying ambient pressure) throughout the launch and ascent phases of flight. Flow expansion is self-adjusted at altitudes lower than design altitude, which improves thrust coefficients and thrust (Naghib, et al., 2006).

At higher altitudes, the operation is almost similar to the conventional nozzles. Likewise, when the exit pressure equals ambient pressure at design altitude, the expansion is optimum or fully expanded. However, at altitudes lower than the design condition, where the exit pressure is lower than the ambient pressure, flow is said to be over expanded because expansion is incomplete and jet plume exiting the nozzle is small, or the jet exit velocity is lower than optimum. Here, the Aerospike self-adjusts its flow expansion by effectively changing the aerodynamic nozzle exit area unbound from the outer end, and thus sufficiently eliminating any back pressure (Kremeyer, et al., 2006). This is what a conventional nozzle is incapable of and surrenders to flow separation in such conditions. While at higher altitudes, above the design condition, the exhaust plume of aerospike nozzle is bigger than the straight column and yet again, its expansion ratio varies (increases) but as is the case of conventional nozzles, such an under expanded flow fails to

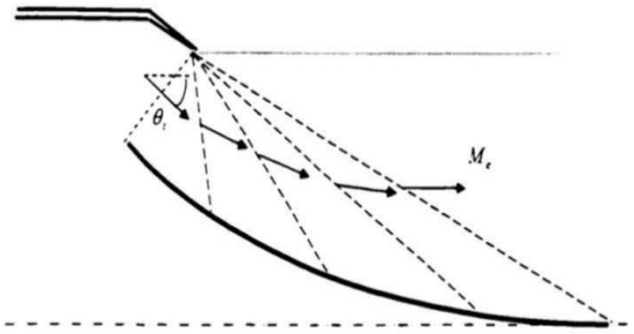

Figure-1: Nozzle Wall Geometry with Expansion Waves

* Institute of Space Technology (IST), Islamabad, Pakistan
** Professor and Head Aeronautics & Astronautics Department, IST, Islamabad, Pakistan. †Email: khanabid62@hotmail.com

influence the pressure distribution at the nozzle wall and, therefore, does not add much to the thrust. Although performance data for aerospike or plug nozzles is always lower than the theoretical expectations but still comparison of the performance during all exhaust plume conditions with conventional nozzles gives it an upper edge (Hagemann, et al., 1998).

Continuous research is being carried out on making the space accessible through the future launch vehicles that must be reusable, lightweight, and maintenance friendly. The goal of achieving an economical and viable future vehicle is not easy and success will mainly depend on the development of an integrated and optimized system. Series of studies have been carried out to meet this desired objective. Not only reduction of airframe weight, improvement in operability, and/or cost reduction will be sufficient to realize the desired goals but development of optimal propulsion system through studies such as the one undertaken in this work are essential and are taking us a step closer to human's dream of space exploration.

2. LINEAR AEROSPIKE NOZZLE

The aerospike nozzle studied in this research comprised three parts, namely the thruster, nozzle wall, and base region. No truncation was applied to keep the work simple, as shown in Figure-2. Moreover, other components such as the turbo-machinery and support structure for the nozzle wall, which are essential parts of an engine, were also neglected. The purpose of these assumptions was to keep the focus of the research on the nozzle analysis, and keep it simple and avoid other complexities of entire engine.

Linear throat of the model (Figure-2), called the thruster, has a rectangular cross-section, whose area is defined in terms of height per unit depth. It is assumed that the thruster has been properly designed and the calculations used to derive the shape of the nozzle assume that at the exit of the thruster, the flow velocity is sonic, i.e., Mach number reaches one. The major thrust contributing section of the engine is the nozzle wall. Exhaust gases leaving the thruster at sonic velocity expand along the nozzle walls until they exit from the engine. Various assumptions have been taken during this work to reduce the complexity of problem, especially the effect of exhaust flow heat on nozzle wall material has been neglected. Moreover, there is no cooling allowance considered as would have been done on an actual engine and base region, it is only formed when truncation is applied, thus introducing wake region and complex aerodynamics. When exhaust flow leaves the nozzle wall, the plume takes the form of an aerodynamic spike aft of the engine. At the corner of the nozzle wall near the exit, flow separates and causes recirculation, which generates pressure on the base. This pressure generates thrust that can approximately account for the complete loss on full length of the ideal spike (Korte, et al., 1997; Niimi, et al., 2003).

2.1 Advantages and Disadvantages

Various significant gains are achieved through the Aerospike nozzles that were considered in 1960s and 1970s for shuttle and in the 1990s for X-33 operations. Some of the obvious merits are as follows:

i) Self-compensation as the launch vehicle climbs through the atmosphere;
ii) Improved thrust coefficient when operating below design pressure;
iii) Application in SSTO vehicles;
iv) Considered better than other advanced nozzles;
v) Aerospike has never flown using liquid propellants;

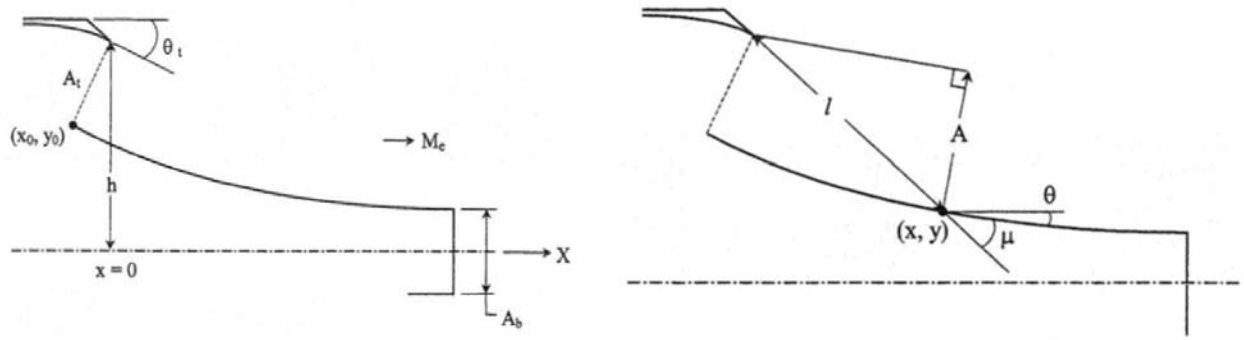

Figure-2: Wall and Flow Geometry Parameters

vi) Smaller in size and lesser in weight;
vii) Thrust vectoring due to the control of individual combustion chambers;
viii) Less risk of failure due to simple turbo machinery; and
ix) Lower vehicle drag due to its compact size and easy integration.

Since aerospike is still a new technological leap, it also has its share of disadvantages, which are a challenge today for the aerospace engineers. These challenges include the lack of proven flight experience, reliability, performance validation (which are expected to happen soon), and manufacturing complexities such as a larger-than-usual surface area, which is subjected to high heat transfer. The termination of Lockheed Martin's X-33 programme in 2001 played an important role in impeding the vigorous development of the aerospike concept.

2.2 Objectives

The objective of this research was to design a MATLAB® code, which can generate an aerospike nozzle contour quickly, correctly and efficiently. For this purpose, an approximate method was used to describe the geometric curves by simple mathematical functions obtained from solving the relevant geometry and aerodynamic relations. The code also calculates the flow properties along the nozzle wall and other performance parameters. Later section, presents an outline of this analytical approach in more details. Next step was to perform a detailed flow field analysis of the design utilizing numerical techniques of a reliable Computational Fluid Dynamics (CFD) software, using the same initial and boundary conditions as in the programme. Complete numerical approach used in this work and the acquired results are deliberated in a separate section. In subsequent part of the paper a comparison of the results acquired through both the approaches in order to verify the assumptions and validate the developed design code is outlined.

3. ANALYTICAL APPROACH

The assumptions listed here and used in this work are similar to those used in the approaches followed by researchers in their published work (Sutton and Biblarz, 2011; Jackson, et al., 1998):

a) Exhaust flow exiting thruster is a steady, inviscid, irrotational, and isentropic, "thus the reflection of waves from the wall, or free boundary are neglected".
b) It is a planar flow, expansion fans are straight lines with sonic conditions at thruster exit or throat.
c) Exit Mach at the nozzle wall is calculated by Prandtl-Meyer function.

The nozzle geometry with its aerodynamic characteristics was elaborated in Figure-1, which clearly shows the thruster angle, θ_t, and the exit Mach number, M_e. The Prandtl – Meyer angle, at exit is set to the deflection or thruster angle where flow is sonic and solved for the exit Mach number as shown in equation (1) and (2):

$$\nu(M_e) = \theta_t = \sqrt{\frac{\gamma+1}{\gamma-1}}\tan^{-1}\sqrt{\frac{\gamma-1}{\gamma+1}(M^2-1)} - \tan^{-1}\sqrt{M^2-1} \quad (1)$$

Where, γ is the specific heat ratio (=1.4).

$$\Delta\theta = \nu(M_e) - \nu(M=1) = \theta_t - 0 = \theta_t \quad (2)$$

The x and y coordinates are given by equation (3) and (4) solving the geometry in Figure-2, which also gives parameters, such as Thruster area A_t, Base area A_b, Flow angle θ, Mach angle μ, and Plume area A, at any point during the flow along the spike.

$$\frac{x}{A_t} = \frac{l}{A_t}\cos(\mu+\theta) \quad (3)$$

$$\frac{y}{A_t} = \frac{h}{A_t} - \frac{l}{A_t}\sin(\mu+\theta) \quad (4)$$

Following definitions apply for above relations:

$$\frac{l}{A_t} = \frac{A}{A_t\sin\mu} \quad (5)$$

$$\frac{A}{A_t} = \frac{1}{M}\left[\frac{2}{\gamma+1}\left(1+\frac{\gamma-1}{2}M^2\right)\right]^{\frac{\gamma+1}{2(\gamma-1)}} \quad (6)$$

$$\mu = \sin^{-1}\left(\frac{1}{M}\right) \quad (7)$$

$$\theta = \theta_t - \nu(M) \quad (8)$$

$$\nu(M) = \sqrt{\frac{\gamma+1}{\gamma-1}}\tan^{-1}\sqrt{\frac{\gamma-1}{\gamma+1}(M^2-1)} - \tan^{-1}\sqrt{M^2-1} \quad (9)$$

The flow properties at each x and y coordinate along the nozzle wall can now be found using the isentropic flow relations:

$$\frac{T_o}{T} = 1 + \frac{\gamma - 1}{2} M^2 \quad (10)$$

$$\frac{p_o}{p} = (\frac{T_o}{T})^{\frac{\gamma}{\gamma-1}} = (1 + \frac{\gamma - 1}{2} M^2)^{\frac{\gamma}{\gamma-1}} \quad (11)$$

$$\frac{\rho_o}{\rho} = (\frac{T_o}{T})^{\frac{1}{\gamma-1}} = (1 + \frac{\gamma - 1}{2} M^2)^{\frac{1}{\gamma-1}} \quad (12)$$

Thrust from each component is calculated separately and superimposed to compute the overall thrust. The thrust generated by both the thrusters is derived from the rocket thrust equation 13:

$$F_1 = 2[\dot{m} u_t + (p_t - p_\infty) A_t] \cos\theta_t \quad (13)$$

Where,
m = Mass flow rate of thruster
p_∞ = Ambient pressure at the design altitude

Using the standard definition for the mass flow rate and thruster exit velocity at sonic conditions, equation 13 becomes:

$$F_1 = 2A^*[p_o \sqrt{(\frac{2\gamma^2}{\gamma+1})(\frac{2}{\gamma+1})^{\frac{\gamma+1}{\gamma-1}}} + p_o(\frac{2}{\gamma+1})^{\frac{\gamma}{\gamma-1}} - p_\infty] \cos\theta_t \quad (14)$$

Equation 15 is used to computed thrust generated by both the nozzle walls:

$$F_2 = -2\int_{x_o}^{L} (p(x) - p_\infty) \frac{dy}{dx} . dx \quad (15)$$

Base region thrust is computed using equation 16:

$$F_3 = (p_b - p_\infty) A_b = 0 \quad (16)$$

Hence, overall thrust from all three components is found through addition of thrust acquired from individual components using equations 14, 15 and 16:

$$F = F_1 + F_2 + F_3 \quad (17)$$

Finally, the thrust coefficient C_F is found using equation 18:

$$C_F = \frac{F}{p_o A^*} \quad (18)$$

3.1 Design Code Input and Output

Design input parameters for linear aerospike are listed in Table-1 using calorically perfect gas properties for propellants with an average combustion chamber pressure of 300 psi. At an ambient pressure of 1.60 psi the nozzle seems to be designed for an operating altitude of approximately 51,000 ft.

Table-1: Aerospike Design Input Parameters

Parameter	Value	Units
Thruster Angle	67.84	degree
Truncation Fraction	1	-
Design Altitude	51,000	ft
Ambient Pressure	1.6	psi
Chamber Pressure	300	psi
Nozzle Pressure Ratio	187.5	-
Specific Heat Ratio	1.4	-
Total Temperature	5,760	R
Throat Size	0.1575	in
Wall Grid Points	100	-

Various output parameters acquired through implementation of analytical programme are listed in Table-2 that include nozzle dimensions and four important performance parameters. The coordinates along the aerospike wall and Mach number at the coordinates are plotted in Figure-3. Whereas, plots given in Figure-4 show the original design code outputs defining the nozzle wall contour in lbs/in^2 (psi), temperature profile in Rankine (R), and density profile in slugs/feet^3 (slugs/ft^3) along the nozzle wall.

Table-2: Aerospike Design Output Parameters

Parameter	Value	Units
Exit Mach	4.16	-
Area Ratio	12.35	-
Exit Height	2	in
Wall Length	8	in
Exit Pressure	1.6	psi
Thrust Coefficient	1.56	-
Thrust	151.06	lbs
Mass Flow Rate	0	slugs/s
Specific Impulse	231	s
Ideal Exhaust Velocity	7,327	ft/s

Also acquired from the design code are the values of thrust coefficient for various nozzle pressure ratios (NPR), i.e., p_o/p_∞, below and above the design value of NPR, which is 187.5 @ 51,000 ft. The graphical relation is plotted in Figure-5.

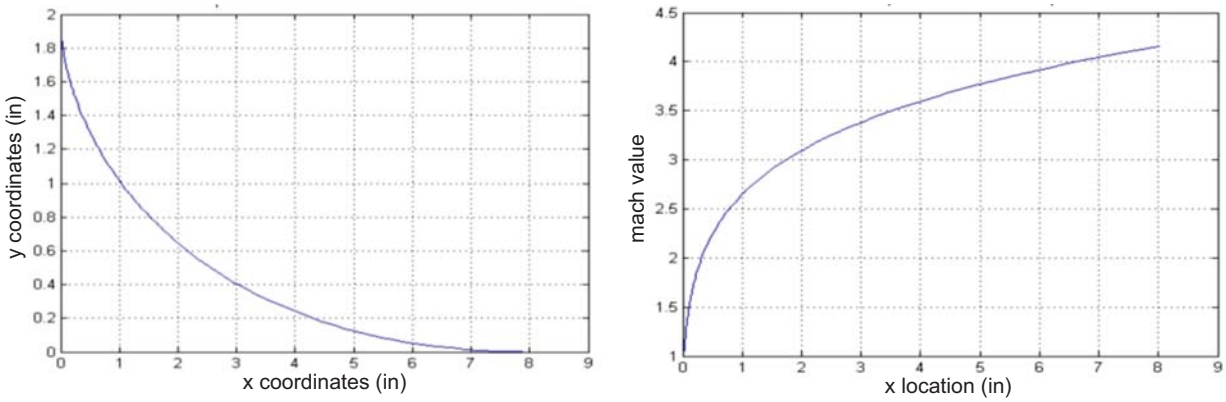

Figure-3: Aerospike Nozzle Wall Coordinates, Mach Profile

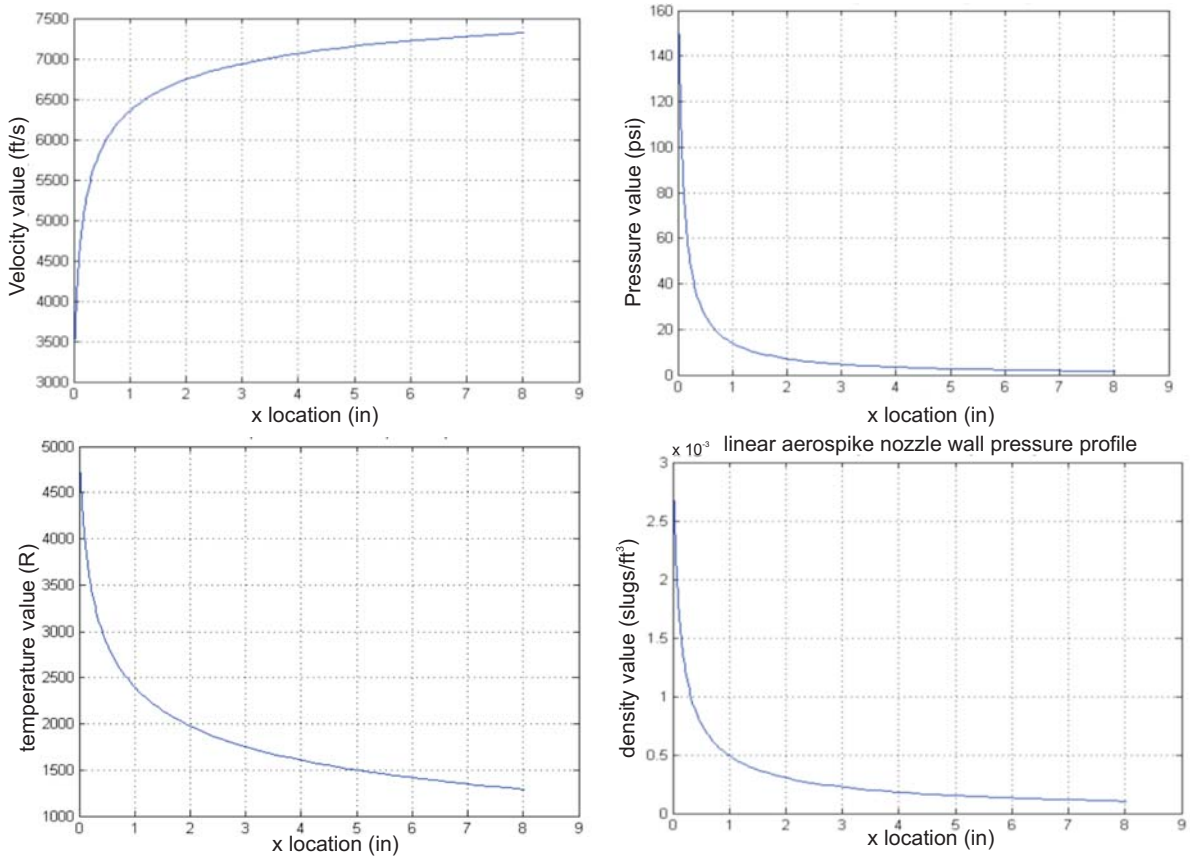

Figure-4: Velocity, Pressure, Temperature and Density Profiles from Analytical Code

4. NUMERICAL APPROACH

The Computational Fluid Dynamics (CFD) commercial tool was used to perform the numerical analysis of the flow through analysis domain. The given flow parameters were used as inflow boundary conditions for the exhaust flow while the ambient pressure was set as the operating condition for each simulation. The model employed first order upwind discretization scheme based on finite difference to solve hyperbolic partial differential equations. The governing equations for the analysis were compressible, two dimensional (2D) and inviscid Euler equations. Thus, the effects due to a thin and attached boundary layer were

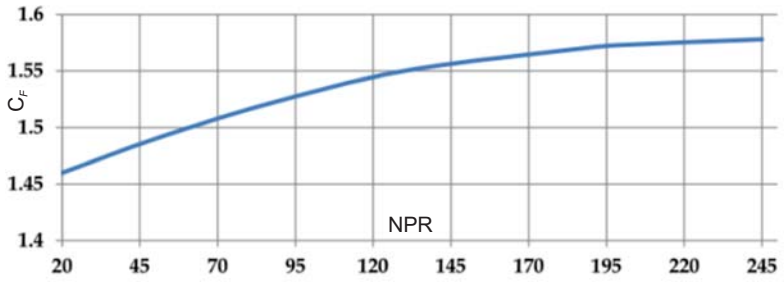

Figure-5: Thrust Coefficient vs. Nozzle Pressure Ratio

Table-3: Solution Method/Controls for CFD

Characteristic	Value
Model	Inviscid (Euler)
Solver Type	Density-based
Time State	Steady
2D Space	Planar
Fluid	Calorically Perfect Gas (γ =1.4)
Formulation Approach	Implicit
Discretization Scheme	First Order Upwind
Courant Number	0.3~1.2
Residuals Absolute Criteria	1.00E-04

neglected, which is justifiable for a case, where the pressure based inertial forces were effectively dominant, with a highly favorable pressure gradient of the nozzle exhaust flow. Solution method and control features adopted for the numerical analysis are tabulated in Table-3.

The set of equation from 19 to 21 depict a conservative form of Euler equations, where;

E = Total energy per unit volume
u = Fluid velocity component in x direction
p = Pressure

$$\frac{\partial \rho}{\partial t} + \nabla.(\rho u) = 0 \tag{19}$$

$$\frac{\partial \rho u}{\partial t} + \nabla.((\rho u) \otimes u) + \nabla p = 0 \tag{20}$$

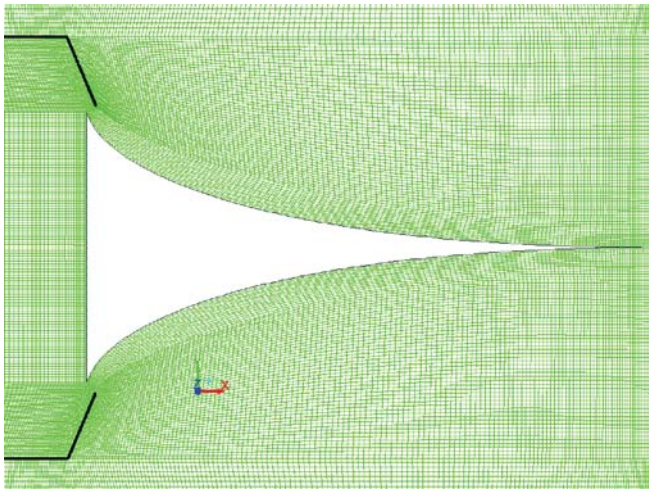

Figure-6: 2D Mesh Model of the Linear Aerospike

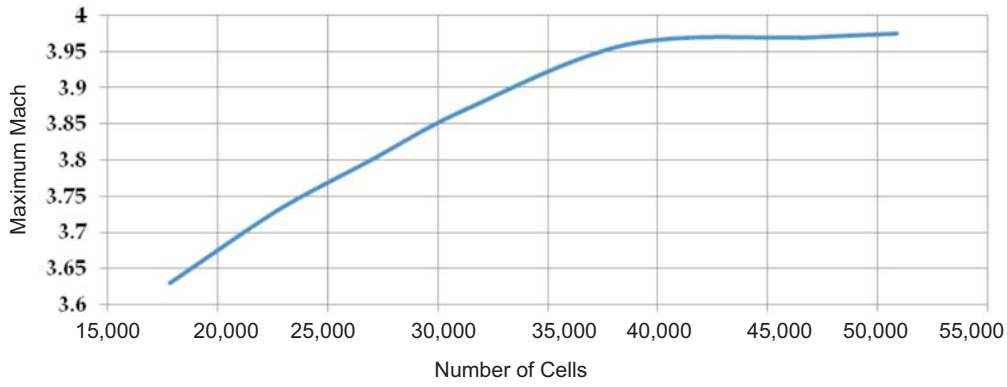

Figure-7: Grid Independence Check

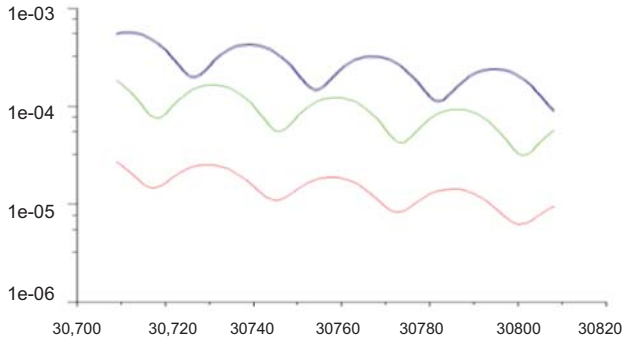

Figure-8: Typical Plot of CFD Residuals

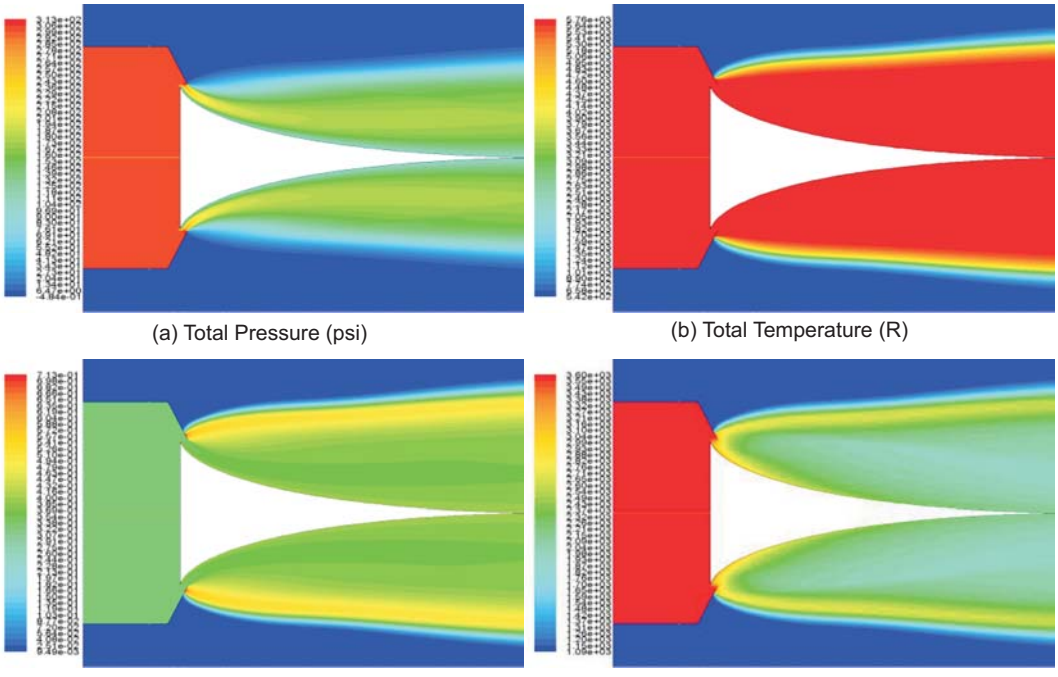

(a) Total Pressure (psi)

(b) Total Temperature (R)

(c) Entropy (btu/lb_m.R)

(d) Speed of Sound (ft/s)

Figure-9: Computational Fluid Dynamics Contours

$$\frac{\partial E}{\partial t} + \nabla.(u(E+p)) = 0 \qquad (21)$$

ρ = Density

To perform the CFD analysis, an input file and a grid generation for the software are essential requirements. The input code created using a Journal file (.jou) format, which contains all database related commands executed while creating a specific model. It also contains all the details of initial/boundary conditions and settings for the CFD analysis.

4.1 Analysis

Selected meshing module from a commercial software was used to create a detailed structured 2D mesh model of the Aerospike assembly comprising cowl, throat, and the full-length spike (nozzle wall), as shown in Figure-6. The mesh used over the 2D model kept significantly finer over the throat and spike to produce improved computational resolution in this area of interest. Multiple grids with increasing cell density with respect to the nodes near the throat and spike region were generated to check for grid-independence in the solution, i.e., no significant

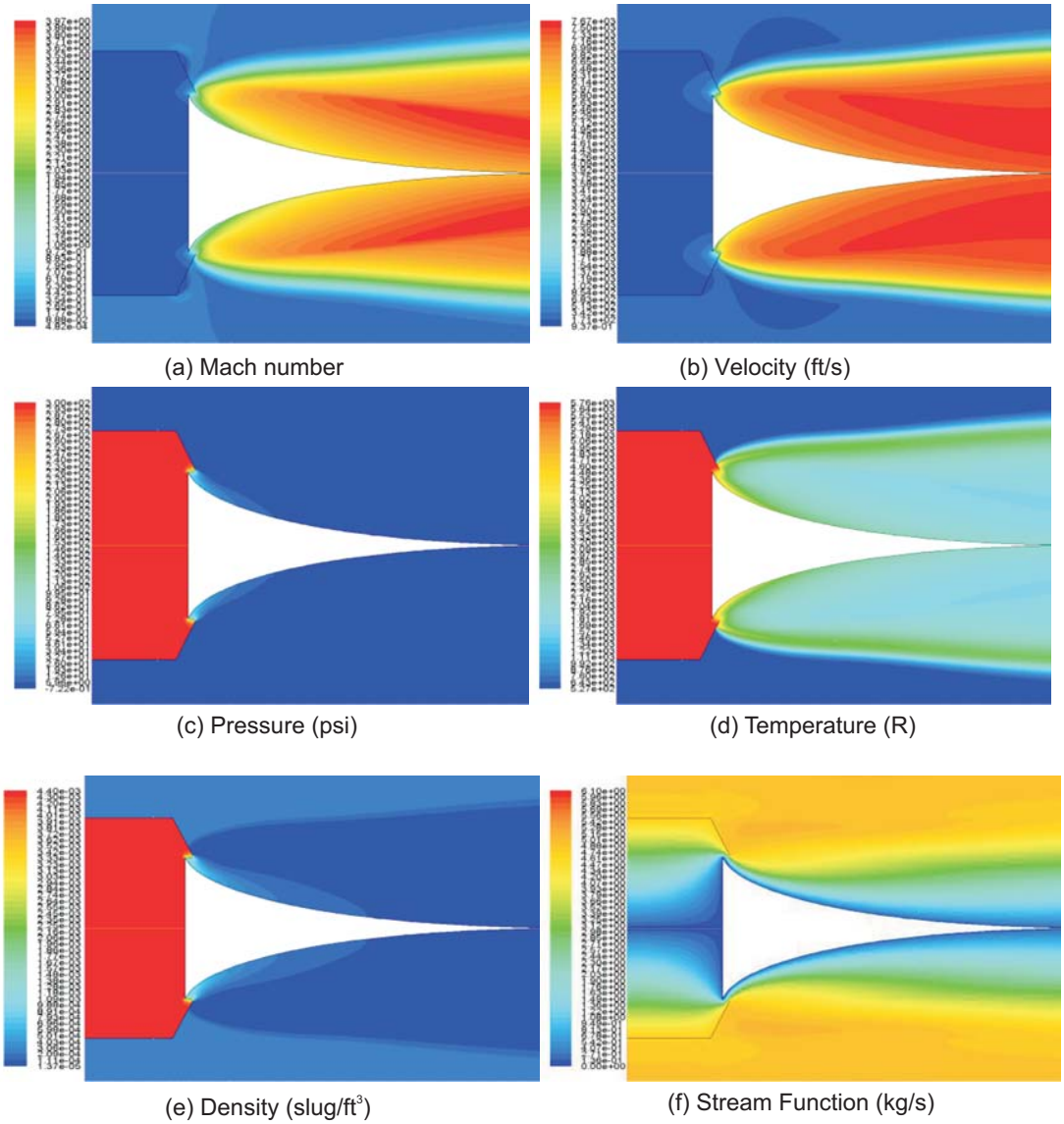

(a) Mach number (b) Velocity (ft/s)

(c) Pressure (psi) (d) Temperature (R)

(e) Density (slug/ft^3) (f) Stream Function (kg/s)

Figure-10: Computational Fluid Dynamics Contours

Table-4: Results Comparison

Parameters	Analytical	Numerical	%
Exit Mach No	4.16	3.46	83.17
Exit Velocity (m/s)	2,233.50	2,235.42	100.01
Exit Pressure (Pa)	11,028.11	9,256.52	83.93
Exit Temperature (K)	710	958	138.7
Exit Density (kg/m^3)	0.054	0.038	70.37
Area Ratio	12.35	12.7	102.8
Mass Flow Rate (kg/s)	4.55	4.86	106.8
Specific Impulse (s)	231	219	94.8
Ideal Exhaust Vel (m/s)	2,233.50	2,158.60	96.6
Thrust (N/m)	667.2	625.4	93.7

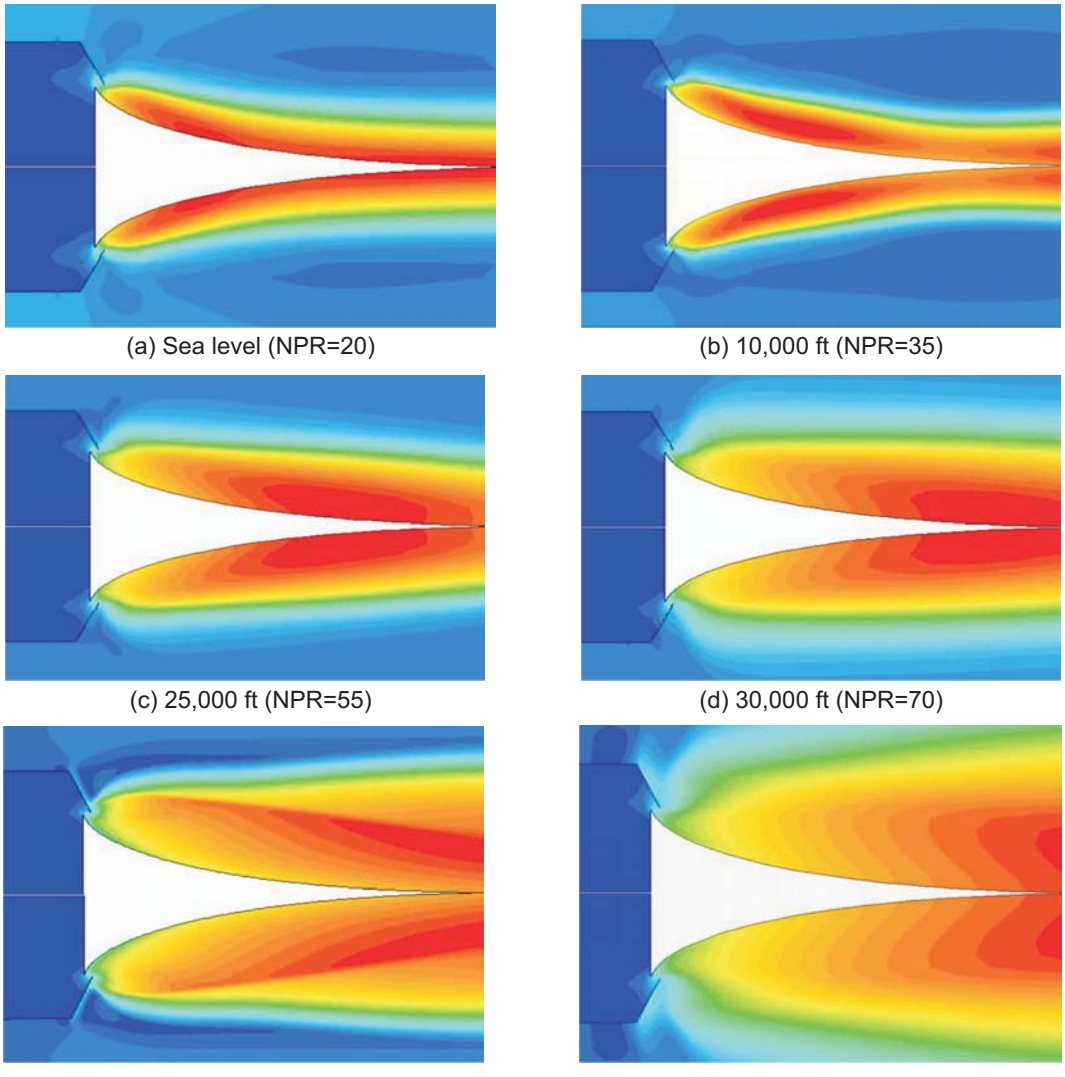

(a) Sea level (NPR=20)

(b) 10,000 ft (NPR=35)

(c) 25,000 ft (NPR=55)

(d) 30,000 ft (NPR=70)

(e) 45,000 ft (NPR=110)

(f) 60,000 ft (NPR=225)

Figure-11: Mach Number Contours at Different Altitudes

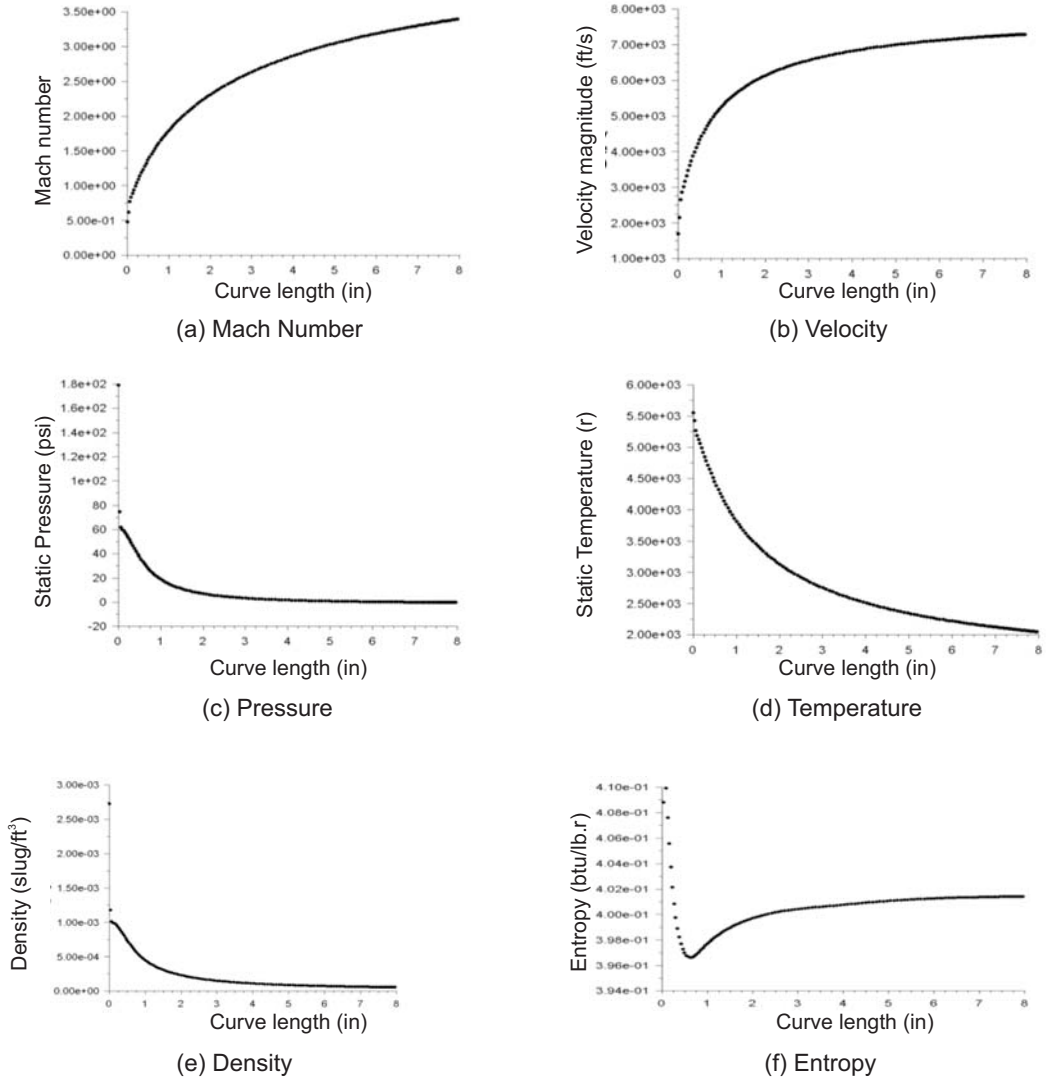

Figure-12: Numerical Flow Profiles

variation in results with increasing cell density.

A code in Glyph file (.glf) format is designed to create several meshes in a very short time. The code is based on tool command language, which allows access to the commands and entities of the used software application. Figure-7 graphically shows the total number of cells for different grids generated via this process and the maximum value of Mach number obtained from their CFD contours inside the relevant domain as an indication of acceptable grid independence. (The percentage difference in the highest Mach number observed in the Mach number contour between the final two grids is a 0.25% increase, which is an acceptable value). Moreover, the flow path trend between any two grids remained completely unchanged, therefore, it is said that a fine grid independence of the solution was achieved, though with more room for improvement. The authors predict that until an infinitely refined mesh is achieved, numerical dissipation, is likely to generate discontinuities.

4.2 Results

In case of valid and reasonable CFD solution, the analysis is expected to converge in addition to being grid independent as discussed above. The residuals for multiple CFD runs showed good convergence from after 8,000 to even 38,000 cycles. A part of a typical

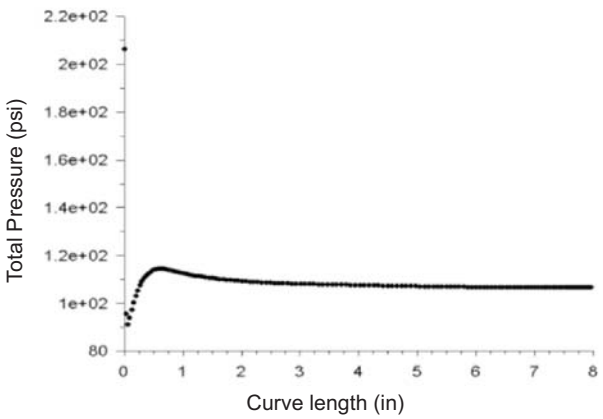

(a) Total Pressure

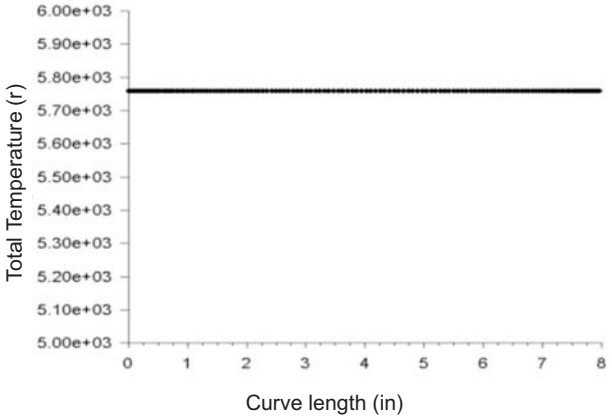

(b) Total Temperature

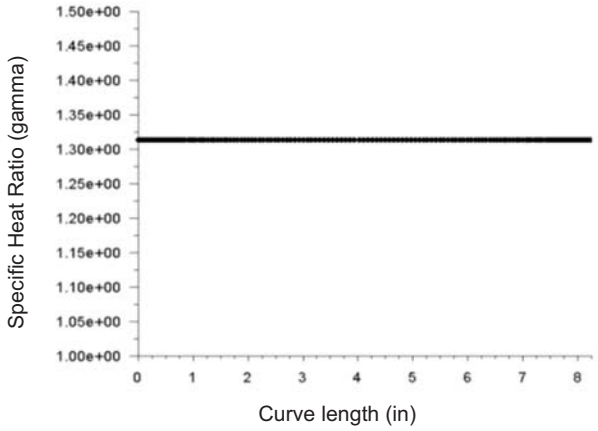

(c) Specific Heat Ratio

Figure-13: Numerical Flow Profiles

CFD residuals plot for the Euler equations is shown in Figure-8. Results acquired from CFD analysis are plotted in Figure-9 to Figure-11 simulated at the design NPR. Mach number contour plots obtained from CFD analysis at different altitudes and NPRs are plotted in Figure-11. The phenomena of over expansion at lower altitudes/NPR and under expansion at higher altitudes/NPR can be clearly seen in these plots.

Flow properties such as Mach number, velocity, pressure, temperature, density and entropy computed along the nozzle wall or spike through CFD analysis at design NPR of 187.5 and altitude of 51,000 ft is plotted in Figure-12. Whereas, total pressure, total temperature and specific heat ratios acquired at same parameters are plotted in Figure-13.

Furthermore, the net mass flow rate for a nozzle of 1 m (i.e., 39.37 in) depth by the CFD analysis was computed to be 0.0052 kg/s, which translates into a valid result.

5. COMPARISON OF RESULTS

The CFD simulations revealed that the exhaust flow exiting the thruster or nozzle throat was approximately independent of the ambient pressure as predicted by the analytical results. Analytical design code outputs including the flow properties at exit plane and the four important performance parameters are compared with CFD results in a tabular form at Table-4. The readers of the paper can clearly note a close similarity between the analytical predictions and numerical solution given the simplicity of the design code utilized and the CFD simulation model chosen. This result would certainly lead one to endorse the applicability and usefulness of the simple approximate method for such a supersonic nozzle contour design.

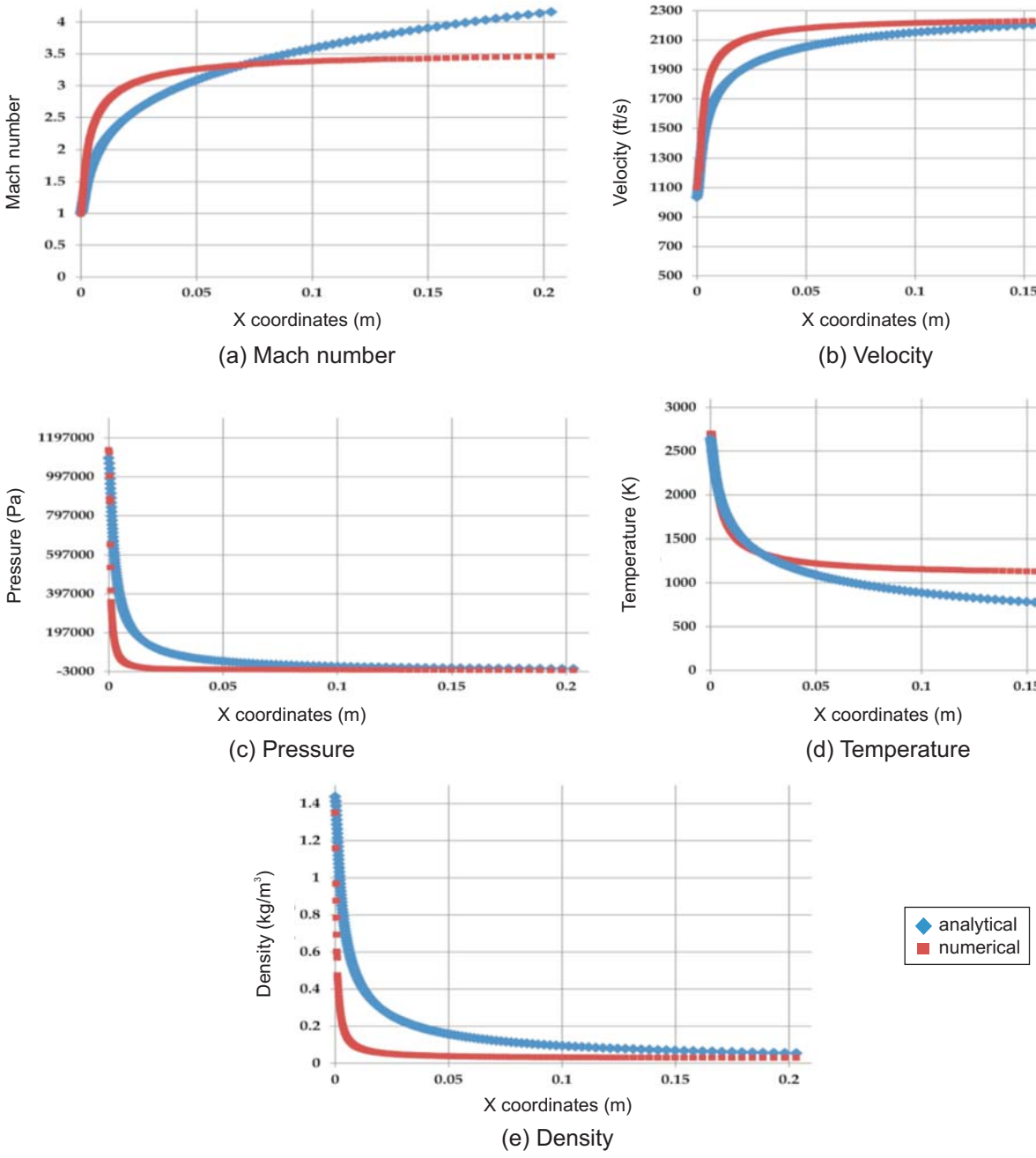

Figure-14: Comparison of Analytical & Numerical Profiles

Though the viscous effects were neglected, the velocity achieved at the exit through CFD is very close to the value predicted by the design programme. This was compromised by the larger mass flow rate through the exit plane and lower specific impulse and thus a slightly lower thrust for a unit depth nozzle.

A comparison of the flow properties acquired both from analytical and numerical results in SI units are plotted in Figure-14. A relatively lower Mach number due to the somewhat higher exit temperature (numerical entropy generation) should not leave the readers in much doubt because the actual numerical exit velocity compensates for it. The reason for this increase of temperature, and pressure, is the generation of shock waves due to numerical dissipation in the CFD

solution. However, the readers should note the adequate resemblance in each of the physical contour lines along the spike length shown in the contour plots of numerical analysis from Figure-10 and Figure-11, which shows the ideal expansion wave characteristics emanating from the thruster exit. This is only in accordance with the theory that along the characteristic lines of expansion waves, the flow properties are indeed continuous. Not to forget that the approximately constant total pressure, total temperature and entropy contours along the spike length in Figure-9 respectively, do satisfy the validity of the isentropic assumptions.

6. CONCLUSIONS

The main purpose of this research was to investigate a quick simple model for a linear aerospike nozzle design from aerodynamic concept. The model includes predictions of nozzle shape, flow properties along the nozzle wall and the four performance parameters at a design condition. The second important step was to prepare a mesh model for the generated contour to and simulate the flow with similar initial and boundary conditions as given and obtained from the design programme. It was observed that the results from the analytical concepts coincided with the numerical tool, thus showing that the proposed approach can be a useful initial/preliminary/simplified engineering path for aerospike rocket design. The main limitation of the research is that, however the analytical code assumed isentropic continuous flow, expansion-shock interaction was seen in numerical results. One of the reasons for their generation could be numerical dissipation (or “artificial viscosity”), but the simple numerical tool used, does not offer shock detection or filter techniques. This can be addressed by employing a highly refined mesh, more advanced CFD software, and more sophisticated solution controls. In case of the experimental data availability, the reliability of the approach may be further validated to realize the development of a propulsion system capable of making its place in reusable future launch vehicles.

REFERENCES

- Bradford, et al., 2000. Exploration of the design space for the ABLV-GT SSTO reusable launch vehicle.
- Bui, T. T., et al., 2005. Flight Research of an Aerospike Nozzle Using High Power Solid Rockets. AIAA Paper 3797.
- Dorsey, J. T., et al., 1999. Airframe integration trade studies for a reusable launch vehicle. Paper read at AIP Conference Proceedings.
- Garvey, J., and Besnard, E., 2004. Development of a Dedicated Launch System for Nanosat-Class Payloads.
- Hagemann, G., et al., 1998. Advanced rocket nozzles. Journal of Propulsion and Power 14 (5):620-634.
- Huebner, L. D., et al., 1995. Experimental results on the feasibility of an aerospike for hypersonic missiles. AIAA paper:95-0737.
- Jackson, J. E., et al., 1998. The control system for the X-33 linear aerospike engine. Paper read at Aerospace Conference, 1998 IEEE.
- Korte, J.J., et al., 1997. Multidisciplinary approach to linear aerospike nozzle optimization. AIAA Paper:97-3374.
- Kremeyer, K., et al., 2006. Computational study of shock mitigation and drag reduction by pulsed energy lines. AIAA journal 44 (8):1720-1731.
- Naghib-Lahouti, et al., 2006. Investigation of the Effect of Base Bleed on Thrust Performance of a Truncated Aerospike Nozzle In Off-Design Conditions. Paper read at European Conference on Computational Fluid Dynamics.
- Niimi, T., et al., 2003. Analyses of flow field structures around linear-type aerospike nozzles using LIF and PSP. Paper read at Instrumentation in Aerospace Simulation Facilities, 2003. ICIASF'03.
- Shtessel, Y. B., and Hall, C. E., 2000. Sliding mode control of the X-33 with an engine failure.
- Sutton, G. P., and Biblarz, O., 2011. Rocket propulsion elements: Wiley. com.
- Tirpak, J. A., and John, A., 1998. The flight to orbit. *A*ir Force Magazine 81:41-45.
- Wang, T. S., 1999. Analysis of linear aerospike plume-induced X-33 base-heating environment. Journal of Spacecraft and Rockets 36 (6):777-783.